International Journal of Pharmaceutics 422 (2012) 462–471

Contents lists available at SciVerse ScienceDirect

International Journal of Pharmaceutics

journal homepage: www.elsevier.com/locate/ijpharm

Erythropoietin-loaded oligochitosan nanoparticles for treatment of periventricular leukomalacia

Ting Wang[a], Yan Hu[b], Michelle K. Leach[c], Long Zhang[b], Wenjing Yang[a], Li Jiang[b], Zhang-Qi Feng[d], Nongyue He[a,*]

[a] State Key Laboratory of Bioelectronics, School of Biological Science and Medical Engineering, Southeast University, Nanjing 210096, China
[b] Teaching and Research Section of Pediatrics, Clinical Medical College, Southeast University, Nanjing 210009, China
[c] Department of Biomedical Engineering, The University of Michigan, Ann Arbor, MI 48109, USA
[d] School of Engineering, Sun Yat-Sen University, Guangzhou 510006, China

ARTICLE INFO

Article history:
Received 31 August 2011
Accepted 27 October 2011
Available online 11 November 2011

Keywords:
Nanoparticles
Oligochitosan
Drug delivery
Erythropoietin
Periventricular leukomalacia

ABSTRACT

In this study, a single intraperitoneal injection of erythropoietin (EPO) loaded oligochitosan nanoparticles (epo-NPs) (average diameter 266 nm) was investigated as a treatment for periventricular leukomalacia (PVL). Nanoparticles were fabricated using a gelation technology process. PVL rats models were prepared to examine the therapeutic efficacy of epo-NPs and analyze the mechanism by which epo-NPs protect white matter. The metabolization of epo-NPs in the liver was also investigated. The pathology and behavioral data show that this single injection of a low quantity of epo-NPs had an excellent therapeutic effect on the rat model of PVL. The EPO release curve in phosphate buffered saline solution was a good fit with the zero-order kinetics distribution and was maintained at around 25% in 48 h. In vivo experiments demonstrated that 50 IU/kg epo-NPs had the same effect as a 5000 IU/kg direct injection of free EPO. Nanoparticles prolonged the time course of EPO metabolization in the liver and the stable release of EPO from the nanoparticles kept the plasma concentration of EPO at around 100 IU/ml during the 8–12 h post-injection. Therefore, we suggest that oligochitosan based nanoparticles are an effective vehicle for drug delivery.

1. Introduction

Research on nano-carrier systems for polypeptide delivery usually focuses on the improvement of therapeutic efficacy and the reduction of side effects (Wu et al., 2009; Min et al., 2008). Hypoxic–ischemic encephalopathy is an important cause of perinatal mortality and permanent neurological morbidities, but specific medications against it are mostly lacking in current medical practice. Erythropoietin (EPO) has been used in the clinic for the hematological diseases (Junk et al., 2002). However, the clinical application of EPO has been associated with undesirable side effects, due to over administration or protease attack. To reduce these side effects and increase the therapeutic effect of EPO, we developed a type of EPO-loaded nanoparticles (epo-NPs) composed of cross linked oligochitosan. These epo-NPs were spherical, highly monodispersed and stable in an aqueous system. Additionally, the use of a natural polymer as the carrier material avoids any potentially toxic effects of synthetically derived nanoparticles (Brownell et al., 2004).

In our study, the therapeutic effect of the epo-NPs was investigated in a rat model of periventricular leukomalacia (PVL). PVL, a form of white matter disease closely associated with cerebral palsy, remains a major problem in premature infants. Increasing evidence has indicated that a hypoxia–ischemia/reperfusion injury plays an important role in PVL. In this study, a rat model of PVL was created through the administration of the toxin 3-nitroproprionic acid (3-NP). The chemical neurotoxicity of 3-NP is associated with preterm birth, neonatal neurological disorders and increased levels of proinflammatory cytokines in amniotic fluid and fetal blood (Arvin et al., 1996; Akopian et al., 2008). EPO is a glycoprotein hormone produced mainly in the renal interstitium in response to hypoxic stimuli. It primarily enhances red blood cell production and additionally has biological effects on endothelial cells (Silva-Adaya et al., 2008; Wei et al., 2006).

EPO is widely used in anemia treatment and also frequently used to increase the hematocrit of patients who have become anemic due to ischemia and hypoxic disease (Mizuno et al., 2008; Mullol et al., 2006). Low concentration of EPO as drug for neural disease was studied in many groups (Mizuno et al., 2008). However, the enhancement of therapeutic efficacy of EPO in clinical treatment is still different to be realized. An EPO carrier is a promising method to increase therapeutic benefit (Wang et al., 2010). In this paper we

* Corresponding author. Tel.: +86 25 83790885; fax: +86 25 83790885.
E-mail address: nyhe1958@163.com (N. He).

0378-5173/$ – see front matter © 2011 Elsevier B.V. All rights reserved.
doi:10.1016/j.ijpharm.2011.10.058

show some results to illustrate the mechanism about how the EPO carriers enhance the curative effect.

Oligochitosan based nanoparticles have been widely investigated in the research field of drug delivery, particularly with respect to the encapsulation of peptides and proteins, because of the excellent biocompatibility and non-immunoreactivity of oligochitosan (Yuan et al., 2008; Li et al., 2009; Cu and Saltzman, 2009; Vila et al., 2004). We designed epo-NPs to protect EPO from protease digestion and prolong the treatment effect on PVL by controlling and prolonging the release of EPO. Drug release, plasma concentrations of EPO and metabolism of epo-NPs in the liver were analyzed to characterize the release time course. Histology experiments, analysis of growth associated protein-43 (GAP-43), MRI experiments and behavior tests were carried out to confirm the therapeutic efficacy of epo-NPs. Our results indicate that epo-NPs protected against the detrimental effect associated with chemical hypoxia and facilitate neuronal survival in the PVL model of postnatal day 5 (P5) rats by enhancement of mitogenesis and biosynthesis in glial cells. So we suggest that epo-NPs are a potential promising therapy for the treatment of PVL.

2. Materials and method

2.1. Materials

Water-solubility oligochitosan (OCS) was purchased from Haidebei Halobios Co., Ltd. (Ji'nan, China). Tripolyphosphate (TPP) was obtained from Sigma–Aldrich (USA). Trypsin–EDTA and EPO were obtained from Sunshine Pharmaceutical Co., Ltd. (Shenyang, China). Phosphate buffered saline (PBS) solution (Sinopharm Chemical Reagent Co. Ltd.) (pH = 7.4) (Shanghai, China) was obtained from Sinopharm Chemical Reagent Co. Ltd. All solvents used in these experiments were analytical grade. All additional chemicals were obtained from Sigma–Aldrich except where otherwise noted.

2.2. Synthesize of EPO-loaded nanoparticles

EPO-loaded nanoparticles were synthesized by ionic gelation of sodium tripolyphosphate (TPP) and oligochitosan (OCS) (Yang et al., 2009). A 1 wt% aqueous solution of EPO was mixed with a 3 wt% aqueous solution of oligochitosan. EPO nanoparticles were obtained upon addition of the TPP solution into the oligochitosan solution at a ratio of TPP/OCS at 1/3 under mild mechanical stirring (550 rpm) at room temperature. Acetic acid was used to keep the pH below 6.5 during reaction. The nanoparticles were collected by centrifugation at 4000 rpm/min and washed three times with ethanol then rinsed with phosphate buffered saline three times. The resulting epo-NPs were then freeze-dried.

2.3. Nanoparticle morphology

The morphology of the nanoparticles was characterized by a scanning electron microscope (SEM) (JEOL JSM-T 220A scanning electron micro-scope, JEOL Ltd., Japan) operating at an accelerating voltage of 10–30 kV. The nanoparticles were sputtered with gold to make them conductive and placed on a copper stub prior to the acquisition of scanning-electron microscope images. The epo-NPs were also observed by transmission electron microscope (TEM). TEM images were taken with a Philips CM-100 Transmission Electron Microscope equipped with a Hamamatsu Digital Camera ORCA-HR operated using AMT software at 50 kV (Advanced Microscopy Techniques Corp., Danver, MA). Samples were prepared by depositing a diluted nanoparticle suspension onto a carbon-coated copper grid which was then air-dried before image acquisition. Dynamic light scattering (DLS, Malvern Instruments Ltd.) was used to determine the size distribution of the nanoparticles.

2.4. EPO release from nanoparticles

The epo-NPs were deliquesced in citrate to check the EPO loading amount and the drug release half life using EPO ELISA kits (Shanghai Blue Gene Biotech Co. Ltd., China). The encapsulation efficiency (EE) of EPO can be calculated by the following formula:

$$\mathrm{EE} = \frac{W_C}{W_G} \times 100$$

W_C: encapsulated EPO quantity and W_G: the gross quantity of EPO

PBS was used as the release medium. Epo-NPs were immersed in PBS solution and stirred at 100 rpm/min at 37 °C. The EE was tested at several points over 72 h by extracting 5 ml of the PBS release medium and replacing it with the same volume of fresh PBS. The release–time curve was then obtained from the EPO kits.

2.5. Metabolization of epo-NPs

Metabolization of epo-NPs in the livers of the 3-NP injured rats was demonstrated by loading the epo-NPs with fluorescein isothiocyanate (FITC). Rats were fed and sacrificed at 4, 8, 12 and 24 h, respectively. The livers were obtained under nembutal anesthesia (40 mg/kg). In brief, after opening the abdominal cavity the suspended livers were fixed by deep frozen (liquid nitrogen) clamp. The frozen tissues were sliced into pieces of 30 μm thickness by a Leica CM1850 Cryostat and then the amount of fluorescence was determined from three slices. The plasma concentrations of EPO were also obtained from these animals and were analyzed by EPO kits and enzyme calibration. All animal procedures were performed under the International Guide for the Care and Use of Laboratory Animals.

2.6. EPO administration

Seventy-two postnatal day 5 (P5) rats were selected from the Clinical Medicine School of the Southeast University and randomly divided into 3 groups: (1) injured group – rats were stereotaxically injected with 3-NP (Wang et al., 2008), and intraperitoneally injected with blank nanoparticles; (2) EPO experimental group – injured rats were treated with direct injection of free EPO (n = 5000 IU/kg) 1 h after encephalic injection of 3-NP; (3) epo-NPs experimental group – injured rats were treated with intraperitoneal injection of epo-NPs (EPO, n = 50 IU/kg) during 1 h after encephalic injection of 3-NP; and (4) control group – stereotaxically injected with PBS and intraperitoneally injected with blank nanoparticles. The wound was sutured after the procedure. Anesthesia was reversed while maintaining analgesia by an intraperitoneal injection of pentobarbital sodium (1 μg/kg). All rats survived the procedure.

2.7. Histology experiments

At 72 h (P8), 9 days (P14) and 27 days (P32) after injection of the nanoparticles, 8 rats in every group were sacrificed by administering an overdose of pentobarbital sodium. They were then transcardially perfused with a brief pulse of PBS (1 ml/g body weight), followed by 4% paraformaldehyde and 0.2% picric acid in 0.1 M sodium phosphate buffer. The brains were removed and post-fixed in the same solution overnight before being immersed in a 30% sucrose solution with 4% paraformaldehyde for dehydration and subsidence.

2.8. Haematoxylin and eosin stains

Consecutive frozen brain sections (30 μm thickness) of P8 and P14 rats were sliced with a freezing microtome and immersed in the PBS and stained with haematoxylin and eosin (H&E). White mater lesions, grey mater lesions and ventricle volume changes were analyzed by direct observation by microscope. The percent volume of the ventricles was calculated by the following equation:

$$\text{Volume of ventricle} = \frac{\text{total volume of left and right ventricle}}{\text{total volume of whole section}} \times 100\%$$

2.9. Analysis of GAP-43

The frozen brain slices of the P14 rats were stained for GAP-43 using the Strept Avidin Biotin Complex (SABC) kit (Wuhan Boster Biological Technology Co.). Image-Pro plus 5.0 was used to analyze the GAP-43 stained images. One field of view was taken at the middle of the callus. Two fields of view at both sides of the cingulum and two more fields of view at both sides of the inner vesicle in the anterior fontanelle at 100× magnification were analyzed.

2.10. MRI experiment

Infant rats were evaluated with one or more magnetic resonance imaging scans according to standard protocol. All scans were high resolution and performed using an animal bed. A PharmaScan 7T was used to acquire MRI data from live rats. Magnetic resonance imaging findings were graded using a validated score (Glass et al., 2008). White matter was considered "normal" if there were no periventricular white-matter abnormalities and areas >3 of T_1 signal abnormality were considered as abnormal white matter injury.

2.11. Behavior test

2.11.1. Open field test

The P32 rats were placed in the centre of an open field (44 cm × 44 cm × 32 cm) under weak red light (40 W) illumination at the same time for the analysis of spontaneous activity. A computer defined grid lines divided the open field into four sides and corner regions, with each grid line being 10 cm from the wall and the central region possessing an area of 576 cm^2 (Choleris et al., 2001). The route, traveled distance, mean velocity (V_{mean}), maximal velocity (V_{max}), number of rearings, and time spent in/number of visits to the central compartment were calculated over a 5 min session. The score for combined locomotor capability was used as a measure of spontaneous activity of the rats.

2.11.2. Resistance test

After being in the open field for 5 min, each rat was quickly picked up by an experimenter wearing a leather glove unfamiliar to the rat (Lin et al., 1993). The rat's resistance to being picked up was scored according to the following 7-point scale adapted from Albert and Richmond (Matute et al., 2007): 0 = does not resist being picked up, 1 = vocalizes or shies away from hand, 2 = shies away from hand and vocalizes, 3 = runs away from hand, 4 = runs away and vocalizes, 5 = bites or attempts to bite, 6 = launches a jump attack at the experimenter's hand. Every group of 8 rats was tested and judged by the 7-levels above.

2.12. Statistical analysis

Statistical analysis was performed using commercially available software (SPSS, version 13.0). Perfusion parameter values were compared between the models of PBS and 3-NP by staining analysis and histopathological fluorescence dyeing. The Pearson correlation coefficient (P) was obtained to determine the degree of correlation in different groups. P values of different groups less than 0.05 were considered as a statistically significant difference.

3. Results

3.1. Characterization of nanoparticles

The average diameter of nanoparticles is mainly determined by the polymer composition. Low molecular weight oligochitosan is synthesized into nanoparticles with controlled size and narrow diameter distribution. The SEM image (Fig. 1 A) and hydrodynamic diameter (DLS) (Fig. 1C) showed that the diameter of nanoparticles were well controlled around 266 nm with uniform size distribution. From TEM image the nanoparticle was transparent and EPO was encapsulated in the nanoparticles as shown in Fig. 1B.

We investigated the release rate of EPO for 48 h in PBS. The release of EPO is abrupt between 2 and 4 h post-injection, then the curve levels off and the release quantity of EPO is around 25% (W/W) in the following 48 h (Fig. 1D). By comparing zero-order kinetics, first-order Erlang distribution and the Retger-peppa drug release model (Table 1), we found that correlation ratio "R" for zero-order kinetics distribution is the largest one (0.944).

3.2. Metabolization of epo-NPs

Metabolization of EPO in the kidney, liver, heart and neural tissue has been demonstrated. Florescent images of liver slices (Fig. 2) showed the presence of FITC loaded epo-NPs in liver. The FITC-loaded epo-NPs (fluorescent spots) were observed 4 h after injection. The nanoparticles were visible in the liver for up to 24 h (Fig. 2D) and large quantity of epo-NPs can be found in liver between 8 and 12 h (Fig. 2B and C) post injection.

These results were supported by Fig. 2E which showed the plasma concentration of EPO in the model of rats during 24 h. From the histogram we found that after direct injection of 5000 IU/kg free EPO the peak value of EPO blood concentration reached 217 IU/ml. Epo-NPs retained the EPO plasma concentration around 100 IU/ml during 8–12 h post-injection. The EPO concentration kept in a high level at 24 h post-injection of the epo-NPs.

3.3. Encephalocoele change

H&E staining were used to evaluate the therapeutic efficacy of epo-NPs on anoxia in rats (Fig. 3A–F). A brain slice of callose from the control group is shown in Fig. 3A where the white matter under the cortex and callose appears healthy. Stereotaxic injection of 3-NP and intraperitoneal injection of blank nanoparticles were used for the rats in the injured group. H&E staining of the injured group (Fig. 3B and E) shows that the white matter under the cortex and callose exhibited serious leukoaraiosis after injection. As shown in Fig. 3B, the ventricles appeared to expand after 3-NP injury. Through calculation, the average ventricle volume of the injured group was abnormally dilated ($P = 0$) compared with the control group and the experimental group ($P < 0.05$). In the experimental group injected with epo-NPs, solidification and cystic lesions in the white matter around the ventricle cannot be clearly found at P8 (Fig. 3C). Additionally, the ventricles of the epo-NPs cured group were more symmetric at P14 (Fig. 3D) compared to the injured group.

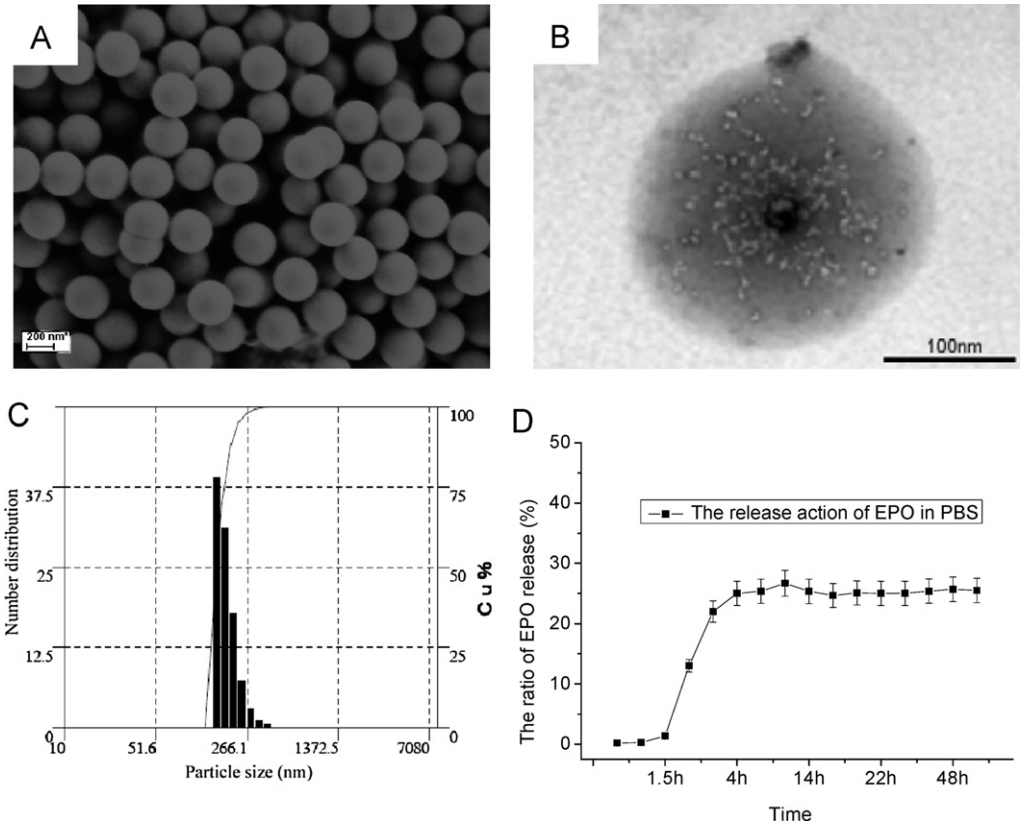

Fig. 1. (A) SEM image of EPO loaded CS-NP; (B) TEM image for EPO loaded CS-NP, the insert clearly shows the EPO protein (the bright spots) encapsulated in the particles; (C) the size distribution of particles; (D) EPO diffused concentration–time curve.

By means of H&E staining, sub-cortical and periventricular white matter rarefaction of P8 rats were observed in the injured group (Fig. 3E). As marked in Fig. 3E, the loose cystic brain tumors and liquefaction of brain were found on the callose, at the same time the cortex and epithelial tissues were seriously damaged compared with the group that received an injection of free EPO (5000 IU/kg) (Fig. 3F). In the epo-NPs group and large quantity of EPO injected group, dilatation of the ventricle has been inhibited.

Compared with the 3-NP injured group, the oligodendrocytes (OLG) (indicated by distinct purple points in H&E stained images) in epo-NPs cured group were healthier and appeared numerous. The reason was that the stable release of EPO from the nanoparticles inhibited the death of oligodendrocytes progenitor cells. The increased presence of OLG leaded to the development of the myelin sheath.

3.4. GAP-43 analysis

Using immunohistochemistry techniques, we examined the expression of neuronal growth associated protein-43 (GAP-43). As a marker of axonal regeneration among cortex, callose, inner vesicle and fornix of P14 rats, the change in GAP-43 was determined by GAP-43 staining of P14 rats as shown in Fig. 4 A and B and Table 2. The positive cells in the 3-NP injured group (Fig. 4B) were fainter than those in the control group (Fig. 4A). At the same time, from Fig. 4A, C and D and Table 2, the number of positive cells in the non-injured control group, epo-NPs injected group and EPO (as free drug) direct injection group were similar. Neuronal growth associated protein GAP-43 will be expressed at high levels during fetal development and axonal phosphorylated. The decrease in the amount of GAP-43 was attributed to the damage caused by 3-NP. Injection of epo-NPs prevented the decrease of immature oligodendrocytes and myelin basic protein. Statistical analyses of average optical density showed obvious damage to positive cells in the injured group due to the action of 3-NP. The Pearson correlation coefficient (P) of GAP-43 expression (Table 2) between the epo-NPs group and 3-NP group was $P < 0.05$, and $P > 0.05$ was obtained between the epo-NPs group and control group. After epo-NPs therapy, positive cells were effectively protected from the 3-NP damage. The brain injury was significantly decreased. The quantity of positive cells in epo-NPs group was similar with the EPO (5000 IU/kg) directly injected group as show in Fig. 4C and D and Table 2.

3.5. Weight changes

The weight differences of the rats were measured to confirm the therapeutic efficacy of epo-NPs. As shown in Fig. 5, we found that the weight of rats injected with 3-NP and blank nanoparticles (the injured group) increased faster than that in the two other groups ($P < 0.05$), which was due to the metabolic disturbances found after

Table 1
The drug release model formulas and correlation ratio "R".

Drug release model	Zero-order kinetics	First order Erlang distribution	Retger peppa
Formula	$y = 0.034\,e^{1.323x}$	$y = 5.635x - 9.534$	$y = 0.093x^{3.115}$
R	0.944	0.827	0.845

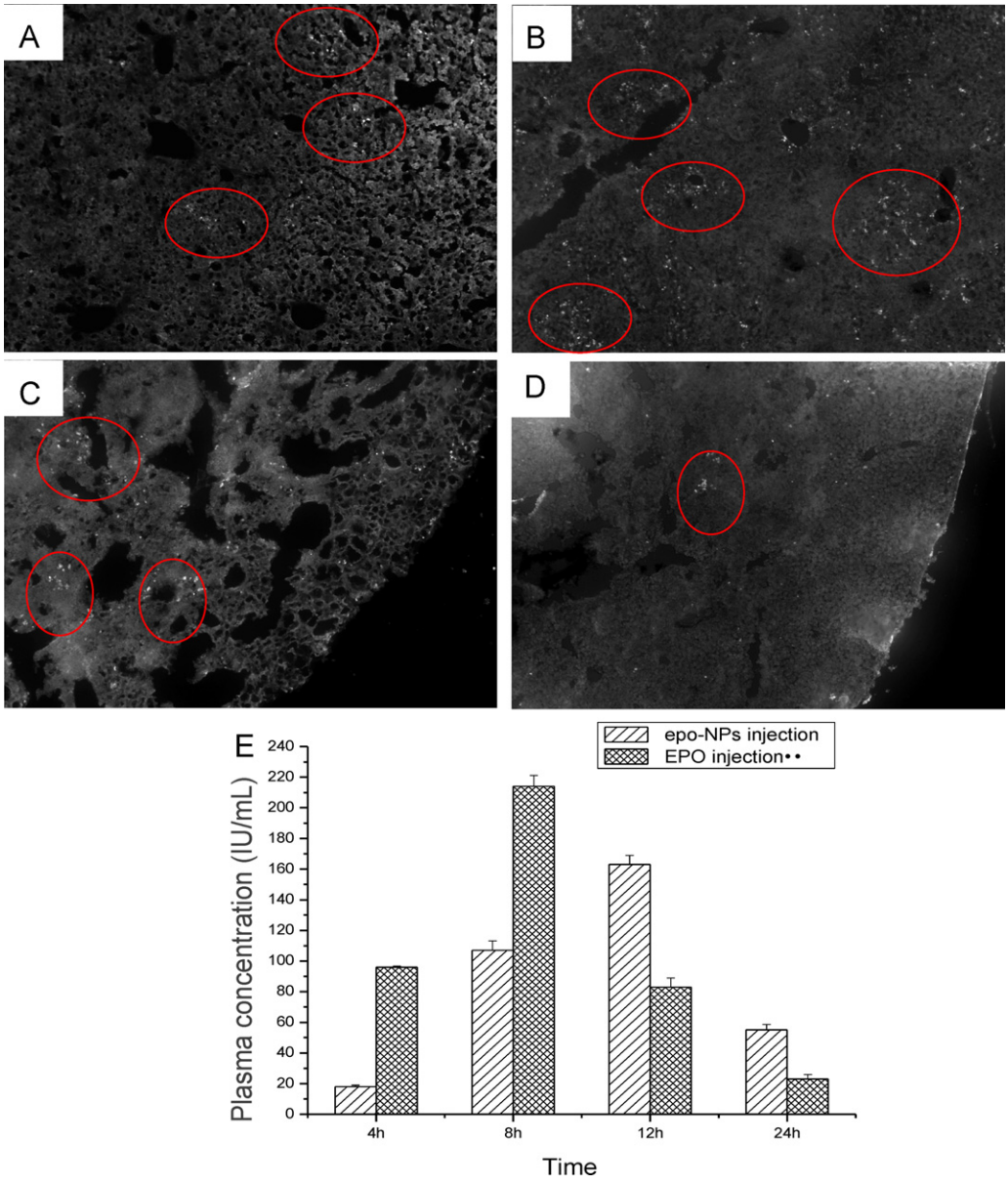

Fig. 2. Metabolism of the particles in liver. (A) 4 h after intraperitoneally injected EPO-NP, quantity of EPO-NP concentrated in the lobules of liver; (B) EPO-NP concentrated around hepatic vein, after 8 h of intraperitoneal injection; (C) 12 h after intraperitoneal injection, and (D) 24 h after intraperitoneal injection; (E) plasma concentration of EPO in blood.

injection of 3-NP. From the results, we suggested that epo-NPs can provide persistent therapy on PVL during the growth of rats.

3.6. Behavioral tests

The rats in the injured group showed significant alterations in response on an open field active behavior assay (Fig. 6). The injured rats showed reduced exploratory behaviors compared with the experimental group ($P = 0.027$, $t = 2.398$). The behavioral activity of rats in the epo-NPs group was significantly better than the injured group ($P < 0.05$) and was similar to the control group (experimental group = 16.37 ± 2.13; control group = 20.25 ± 3.61). Higher levels of cerebrum paralysis mainly lead to decreases in behavioral ability as judged by this test.

The rat-resistance test (Albert, 1975) showed that the injured group had less resistant reactions to being picked up than the experimental group. The average score of the anoxemic rats in the injured group was 7.62 (Fig. 6), while the scores of the rats in

Table 2
The number of positive GAP-43 cell ($x \pm s$, $n = 6$).

P30	3-NP	EPO-NPs	EPO	PBS	*F*
GAP-43	21.67 ± 8.48[a]	43.83 ± 7.46[a,b]	41.53 ± 6.47[b]	56.67 ± 9.52[b]	20.663

[a] Rats injected with epo-NPs compare with 3-NP injured group $P < 0.05$.
[b] Rats injected with epo-NPs compared with the EPO direct injection group and compared with control group, $P > 0.05$.

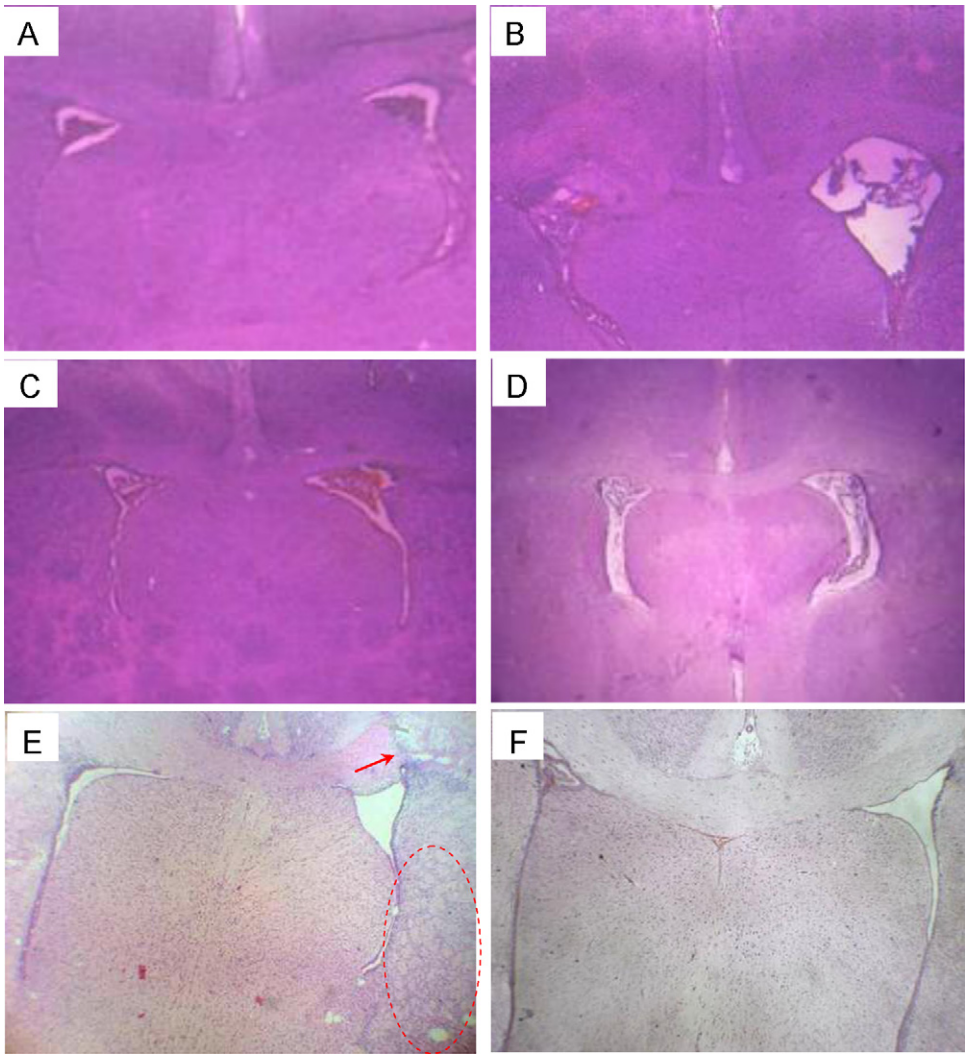

Fig. 3. (A) Control group injected with PBS and blank nanoparticles of P8 rats (100×), ventricle on both sides of cerebral hemisphere are well-balanced; (B) the P8 rats injected with 3-NP and blank nanoparticles (100×). Loose white matter and callose among cortex, coagulation necrosis and cystoid pathological changes can be found; (C) the group with injections of 3-NP and EPO-NPs in P8 (100×), ventricles change seems to be prohibited; (D) the group with injections of 3-NP and EPO-NPs in P14 (100×), ventricles change seems to be prohibited; (E) the rats just injected with 3-NP. Tissue edema, anemic infarct can be found as marked in image; (F) free EPO (5000 IU/kg) treated rats.

the experimental group and control group were 16.15 and 17.23, respectively. Neurotoxicity of 3-NP was responsible for the decreased resistance. The treatment of epo-NPs elevated the score to 16.15 which was very similar to the rats in the control group.

3.7. MRI analysis

From the MRI analysis, it was found that the brain of rats in both the control group and the experimental groups were normal. Moreover, no atrophy of cortex or loss of white matter appeared from the results of MR scanning images as shown in Fig. 7C and D. Fig. 7E (T1W1) and F (T2W2) shows that coagulation necrosis affected the periventricular white matter of rats significantly in the injured group.

4. Discussion

4.1. EPO release

Oligochitosan based NPs have been used to improve the cell internalization or intracellular trafficking of proteins and peptides. Oligochitosan nanoparticles possess many excellent characteristics such as biodegradability, biocompatibility and non-immunoreactivity which are beneficial to the application of these particles in the field of drug delivery, as well as diagnostics and therapy of disease. In the present study, TPP was used as a cross linking agent which leads to the formation of oligochitosan nanogels. EPO proteins could be observed in the center of the nanoparticles. These results indicate that we fabricated the epo-NPs successfully. Oligochitosan is a permeable and degradable material. PBS medium decreased the concentration of cationic amido in the epo-NPs by alkaline phosphate group, therefore polyelectrolyte complexes of nanoparticles became unstable and there was a gradual decrease in cross linking density. From the EPO release curve and data analysis (Fig. 1D and Table 1) we deduced that release of EPO from 0 to 1.5 h is due to the effusion of EPO from nanoparticles. After 3 h, the EPO release curve exhibited a consistent and stable tendency because a constant quantity of EPO was exposed at the surface of the nanoparticles due to the constant effusion speed of EPO (Fig. 1D). In conclusion, penetration of PBS into the nanoparticles decreased the cross-linking density of the polyelectrolyte complexes, leading to a release of EPO after the initial abrupt increase of the signal.

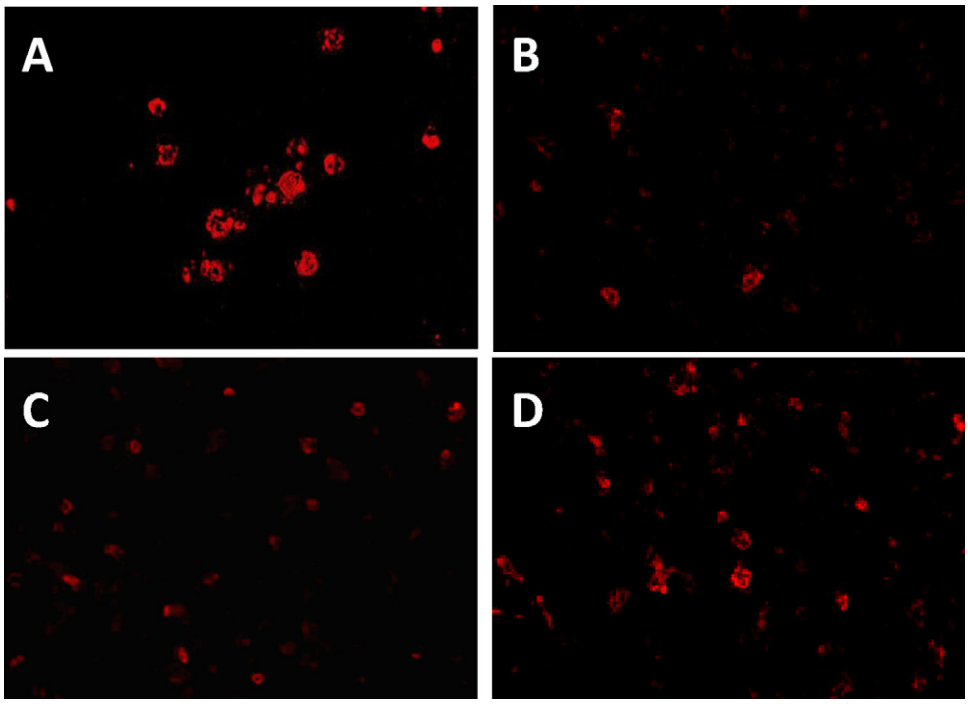

Fig. 4. Fluorescence images of immunoassay staining for (A) controlled group (100×); (B) 3-NP injured group (100×) and (C) experimental group I: free EPO injected group (100×); (D) experimental group II: epo-NPs cured group. Red fluorescent points are growth associated protein-43 (GAP-43) in different groups (100×).

4.2. Metabolization of epo-NPs

Nanoparticles with fluorescent dye were used to demonstrate the activity of epo-NPs in vivo. It is a useful experimental tool for assessing nanoparticle function in hepatic tissues where EPO expression levels were unknown. We chose the liver as the tissue to analyze and used fluorescent dye particles to detect the presence of epo-NPs for the two following reasons: first, almost all of the blood that leaves the stomach and intestines must pass through the liver before reaching the rest of the body and secondly, over 90% of EPO is metabolized in the liver. Additionally, the treatment effect of EPO and the immature livers of newborn rats injured with 3-NP are more sensitive to EPO than the mature livers of adults.

The study of free EPO injection showed that EPO was completely cleared from the blood in 12 h and the peak value of free EPO monomer in the blood appeared at 8 h after injection. The peak value of EPO plasma concentration was delayed to 12 h after protected by epo-NPs compared with free EPO (5000 IU/kg) direct injection. Metabolization of epo-NPs in the liver exhibited that the EPO had a longer plasma half-life when delivered as a nanoparticle formulation than as a free drug.

4.3. Pathology change

The purpose of this study was to evaluate the therapeutic effect of low quantity EPO that loaded with nanoparticles. Sustained injection of EPO has been reported an effective therapy for brain injured rats (Kumral et al., 2003, 2007). EPO was also shown to

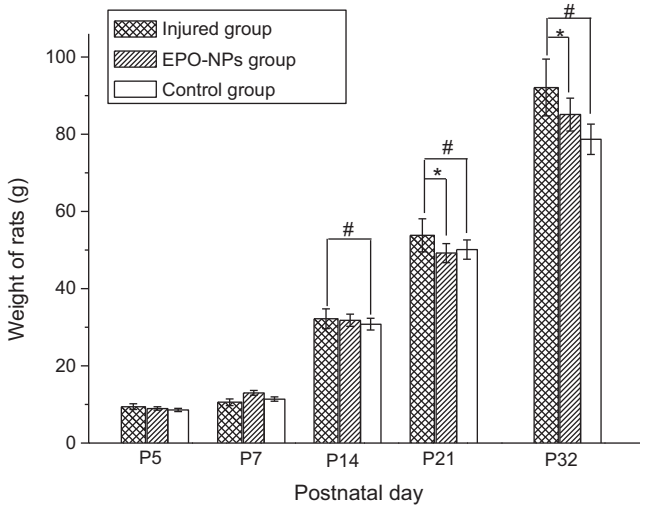

Fig. 5. Body weight changes of rats under the influence of 3-NP and epo-NPs. Injured group grow faster compared with control group, "*" is $P < 0.05$, "#" is $P > 0.05$. Rats in experiment group injected with epo-NPs have similar weight to that of control group.

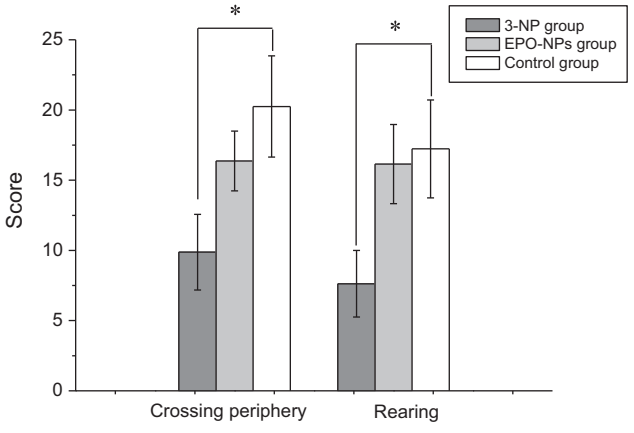

Fig. 6. Histograms show the number of crossings (from one section to another) and the number of rearing of the front paws and of half rotations (180° turns) in three different groups. Tests were initiated at P30. Each animal was monitored for 5 min in open field apparatus. Data are mean ± t ($n = 8$ per group). $^{*}P \leq 0.05$ between the injured group and EPO treated group.

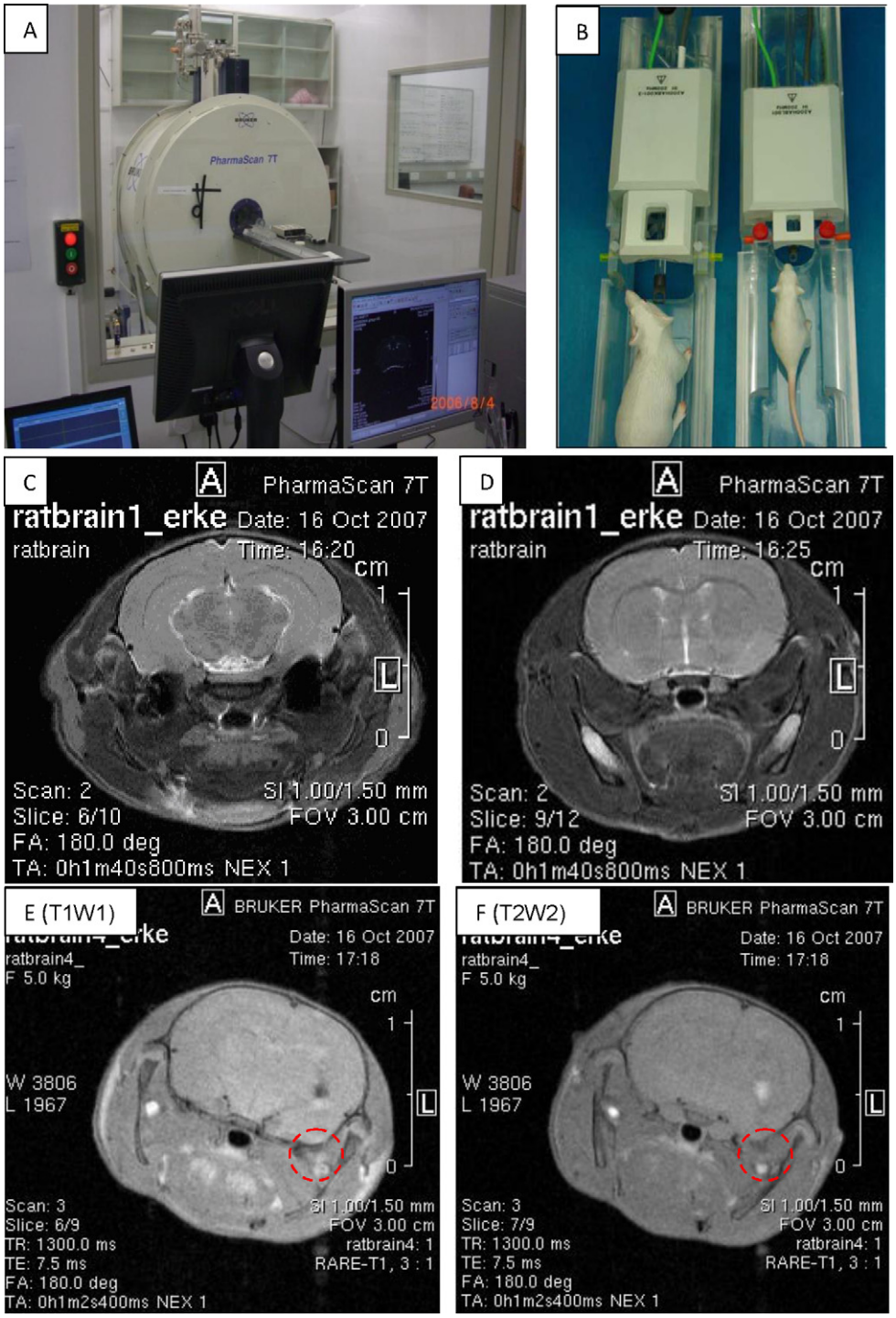

Fig. 7. MRI images of the live rats on the day of P9. (A) PharmaScan 7T; (B) animal bed; (C) the ventricles on the both sides of the rat's brain are healthy in control group; (D) the ventricles of rats in experiment group are almost similar to that of control group after administration of epo-NPs; (E and F) for the injured group, loss of white matter can be observed on the right side, in lateral ventricle. T1W1 image in the left shows low signal and T2W2 image in the right shows high signal, this result is from loss of white matter under 3-NP injuring.

protect neurons against ischemia-induced cell death (Masahiro et al., 2007). EPO treatment can protect brain from infarct and reduce apoptosis of neurons under conditions of hypoxia (Iwai et al., 2007). EPO has been demonstrated in the prevention of PVL in the human infant brain, and may play a role in mediating fetal or neonatal brain injury by 3-NP (Liu et al., 2008). In vivo studies illustrated that 5000 IU/kg EPO injection maintained a plasma drug concentration about 200 IU/ml. It was an effective therapy for brain injury in rats (Vaziri et al., 1995). But in our work, 50 IU/kg EPO loaded in nanoparticles protected rat brain from loss of white matter. From Figs. 3 and 4 we found that the pathology change of brain slices were similar with intraperitoneal injection of 5000 IU/kg free EPO or 50 IU/kg epo-NPs.

The low quantities of EPO delivered as a nanoparticle formulation can avoid many of the side effects caused by the current large quantity of EPO used in clinical treatment of PVL, such as brain damage from stroke and heart attack due to an over increase of the hematocrit. However, the therapy mechanisms about EPO on

3-NP-induced PVL in immature rat brain are still unknown. In the present study, we investigated the effect of postnatal EPO treatment on 3-NP induced PVL injury. We observed a higher expression of GAP-43 in the newborn rat brains after EPO therapy, which indicated that the development of axons in the brain was protected by postnatal administration of epo-NPs.

EPO plays a role in the promotion of cell survival signaling cascades, up regulation of the expression of anti-apoptotic proteins (Aluclu et al., 2007), modulation of intracellular calcium metabolism (Kakhana et al., 2005), attenuation of NO production, inhibition of glutamate release (Catania et al., 2002), and has shown anti-apoptotic, anti-oxidative and anti-inflammatory actions. The neuroprotective effect of EPO on hypoxic–ischemic brain is mediated by distinct mechanisms involving several processes including decreased production and/or release of tissue-injuring molecules such as reactive oxygen and nitrogen species and glutamate, modulation of neurotransmission, reversal of vasospasm, attenuation of apoptosis and modulation of inflammation (Spandou et al., 2005).

We studied treatment with epo-NPs attenuated 3-NP induced injury to myelination in the neonatal rat brain. The protective effect of epo-NPs on anoxemic neonatal rat brain was associated with its ability to keep the plasma concentration of EPO. EPO quantities around 100 IU/ml reduce the expression of inflammatory cytokines and cell death, and increase GAP-43 expression. In particular, the administration of EPO-loaded nanoparticles can avoid EPO break down by proteases, prolong the protective effect of EPO on injured brain, improve the pharmacy effect and decrease the quantity of EPO administration necessary.

4.4. Behavior testing

3-NP has preferential toxicity to cultured striatal, hippocampal, septal, and hypothalamic neurons in vivo. The results in the open field testing and resistance testing indicated that the scores of the rats are significantly influenced by 3-NP injury and EPO therapy. In open field testing, injured rats showed reduced exploratory behaviors compared to the EPO treated group. In resistance testing, rats with 3-NP injury did not resist being picked up and were torpid in the open field test. The results of this behavior testing were in accordance with the pathology study, the rats injured with 3-NP had lost white matter (Fig. 3E) and expressed less GAP-43 positive cells (Fig. 4B).

From the pathology results, we found that higher expression levels of GAP-43 inhibit the death of oligodendrocyte progenitor cells, since a certain quantity of EPO releasing from epo-NPs. Large quantities of oligodendrocytes led to full-growth of the myelin sheath. The fully developed myelin sheath resulted in active and sensitive behaviors of the rats. Thus, it was likely that the quantity of GAP-43 cells was a major determining factor of sensitive action and short time memory of rats. In addition, the data presented also suggest that the erythropoietic system can be used to inhibit systemic inflammation. Our study gives insight into a treatment by EPO loaded nanoparticles that may open a new window of therapeutic opportunities for these critically ill patients.

5. Conclusion

This work focused on the therapeutic efficacy of epo-NPs which played a pivotal role in preventing neonatal cerebral hypoxic–ischemic brain injury. When loaded into OCS/TPP nanoparticles, the quantity of EPO that was necessary for therapy was reduced to 1% of the amount necessary when EPO was administered in free form. The epo-NPs remained in the liver during the 24 h post injection and slowly released EPO, which was still present in the blood at high concentrations at 24 h. The results of pathology testing showed that injection of epo-NPs can attenuate liquefaction and softening of the brain tissue to the same extent as a direct injection of free 5000 IU/kg EPO. Also, behavioral experiments showed that injured rats treat with low quantity of epo-NPs retained good memory and agility. However, further studies will be required to deeply understand the therapeutic mechanism of drug-loaded oligochitosan nanoparticles. Once these queries are overcome, OCS/TPP nanoparticles will likely play an important role in the clinical administration of other types of drugs.

Acknowledgements

We gratefully acknowledge the support to this research from National Key Program for Developing Basic Research (Nos. 2007CB936104 and 2010CB933903) and the 863 High Tech Project (Nos. 2007AA022007 and 2007AA021905), the National Natural Science Foundation (No. 60927001). The authors gratefully acknowledge funding from the "100 Talents Program of Sun Yat-Sen University".

References

Akopian, G., et al., 2008. Decreased striatal dopamine release underlies increased expression of long-term synaptic potentiation at corticostriatal synapses 24 h after 3-nitropropionic-acid-induced chemical hypoxia. J. Neurosci. 28, 9585–9597.
Aluclu, M.U., et al., 2007. Evaluation of erythroprotein effects on cerebral ischemia in rats. Neuroendocrinol. Lett. 28, 170–174.
Albert, A., 1975. Outline Studies in Biology the Selectivity of Drugs. Wiley, London, UK, p. 64.
Arvin, B., et al., 1996. The role of inflammation and cytokines in brain injury. Neurosci. Biobehav. Rev. 20, 445–452.
Brownell, A.L., et al., 2004. 3-Nitropropionic acid-induced neurotoxicity – assessed by ultra high resolution positron emission tomography with comparison to magnetic resonance spectroscopy. J. Neurochem. 89, 1206–1214.
Catania, M.A., et al., 2002. Erythropoietin prevents cognition impairment induced by transient brain ischemia in gerbils. Eur. J. Pharmacol. 437, 147–150.
Cu, Y., Saltzman, W.M., 2009. Mathematical modeling of molecular diffusion through mucus. Adv. Drug. Deliv. Rev. 61, 101–114.
Choleris, E., et al., 2001. A detailed ethological analysis of the mouse open field test: effects of diazepam, chlordiazepoxide and an extremely low frequency pulsed magnetic field. Neurosci. Biobehav. Rev. 25, 235–260.
Glass, H.C., et al., 2008. White-matter injury is associated with impaired gaze in premature infants. Pediatr. Neurol. 38, 10–15.
Iwai, M., et al., 2007. Erythropoietin promotes neuronal replacement through revascularization and neurogenesis after neonatal hypoxia/ischemia in rats. Stroke 38, 2795–2803.
Junk, A.K., et al., 2002. Erythropoietin administration protects retinal neurons from acute ischemia-reperfusion injury. PNAS 99, 10659–10664.
Kakhana, K., et al., 2005. Calmodulin physically interacts with the erythropoietin receptor and enhances Jak2-mediated signaling. Biochem. Biophys. Res. Commun. 335, 424–431.
Kumral, A., et al., 2003. Neuroprotective effect of erythropoietin on hypoxic–ischemic brain injury in neonatal rats. Biol. Neonate 83, 224–228.
Kumral, A., et al., 2007. Erythropoietin attenuates lipopolysaccharide-induced white matter injury in the neonatal rat brain. Neonatology 92, 269–278.
Liu, X.B., et al., 2008. Therapeutic strategy of erythropoietin in neurological disorders. CNS Neurol. Disord. Drug Targets 7, 227–234.
Lin, L.F.H., et al., 1993. GDNF – a glial-cell line derived neurotrophic factor for midbrain dopaminergic-neurons. Science 260, 1130–1132.
Li, Y., et al., 2009. Drug permeability and mucoadhesion properties of thiolated trimethyl chitosan nanoparticles in oral insulin delivery. Biomaterials 30, 5691–5700.
Min, K.H., et al., 2008. Hydrophobically modified glycol chitosan nanoparticles-encapsulated camptothecin enhance the drug stability and tumor targeting in cancer therapy. J. Control. Release 127, 208–218.
Mizuno, K., et al., 2008. Pretreatment with low doses of erythropoietin ameliorates brain damage in periventricular leukomalacia by targeting late oligodendrocyte progenitors: a rat model. Neonatology 94, 255–266.
Mullol, J., et al., 2006. Effect of desloratadine on epithelial cell granulocyte-macrophage colony-stimulating factor secretion and eosinophil survival. Clin. Exp. Allergy 36, 52–58.
Matute, C., et al., 2007. P2X(7) receptor blockade prevents ATP excitotoxicity in oligodendrocytes and ameliorates experimental autoimmune encephalomyelitis. J. Neurosci. 27, 9525–9533.
Masahiro, N., et al., 2007. Modulation of the mitochondrial permeability transition pore complex in GSK-3 beta-mediated myocardial protection. J. Mol. Cell Cardiol. 43, 564–570.

Silva-Adaya, D., et al., 2008. Excitotoxic damage, disrupted energy metabolism, and oxidative stress in the rat brain: antioxidant and neuroprotective effects of L-carnitine. J. Neurochem. 105, 677–689.
Spandou, E., et al., 2005. Erythropoietin prevents long-term sensorimotor deficits and brain injury following neonatal hypoxia–ischemia in rats. Brain Res. 1045, 22–30.
Vaziri, N.D., et al., 1995. In vivo and in vitro pressor effects of erythropoietin in rats. Am. J. Physiol-Renal. 269, F838–F845.
Vila, A., et al., 2004. Low molecular weight chitosan nanoparticles as new carriers for nasal vaccine delivery in mice. Eur. J. Pharm. Biopharm. 57, 123–131.
Wang, T., et al., 2008. Neurotoxicological effects of 3-nitropropionic acid on the neonatal rat. Neurotoxicology 29, 1023–1029.
Wang, T., et al., 2010. Erythropoietin nanoparticles: therapy for cerebral ischemic injury and metabolism in kidney. Nano Biomed. Eng. 2, 46–61.
Wu, P., et al., 2009. Novel methotrexate delivery system based on chitosan–methotrexate covalently conjugated nanoparticles. J. Biomed. Nanotechnol. 5, 557–564.
Wei, L., et al., 2006. Cell death mechanism and protective effect of erythropoietin after focal ischemia in the whisker-barrel cortex of neonatal rats. JPET 317, 109–116.
Yang, W.J., Wang, T., He, N.Y., 2009. Preparation and property of chitosan/sodium tripolyphosphate microcapsules as drug carrier. Chem. J. Chinese Univ. 30, 625–628.
Yuan, X.B., et al., 2008. Preparation of rapamycin-loaded chitosan/PLA nanoparticles for immunosuppression in corneal transplantation. Int. J. Pharm. 349, 241–248.